Energy Technology
Generation, Conversion, Storage, Distribution
www.entechnol.de

In-Depth Analysis of the Internal Energy Conversion of Nuclear Batteries and Radiation Degradation of Key Materials

*Tongxin Jiang, Zhiheng Xu, Caifeng Meng, Yunpeng Liu, and Xiaobin Tang**

Low conversion efficiency and energy output are the main factors hindering the application of the radioluminescent nuclear battery in space. This study analyzes the energy conversion process and proposes a solution of performance promotion. It is found that the energy conversion efficiency of the photovoltaic units is enhanced with increasing incident light intensity. The efficiency of the AlGaInP unit is stable at 22% when the incident energy is at least 3 μW. As for the GaAs unit, the incident threshold value of the photovoltaic response sensitivity is greater than 120 μW. The overall efficiency of the radioluminescent nuclear battery is only 0.37%, consisting of an AlGaInP unit loaded with a low activity ^{63}Ni and the ZnS:Cu phosphor layer. The efficiency increases to 0.87% when an electron radiation source with 270.27 mCi cm^{-2} is adopted. Moreover, the intense intensity source constitutes an extremely electromagnetic pulse radiation environment, which cause the batteries to fail. The radiation damage is introduced to the phosphor layer by radiation sources, producing agglomerations and cracks on the surface and resulting in the transmittance reduction. This study provides guidance for improving the electrical property and optimization solutions of radioluminescent nuclear battery.

1. Introduction

The universe exploration of humans has never stopped. The future development of the aerospace field is breaking through the solar system and entering a wider world.[1] Therefore, stricter requirements on the energy supplements are put forward. In addition to the power requirement for propulsion in spacecrafts,[2] small-volume batteries with sustainable power and stable output are needed to meet the various demand of electronic devices.[3] At present, the main energy source of spacecrafts is still solar energy.[4] However, the solar radiation decreases dramatically as the spacecraft moves away from the solar system.[5,6] Nuclear battery, as a device for collecting the decay energy of radioisotopes, has strong environmental adaptability, stable output power, and high energy density. Therefore, it has the advantages of strong durability,[7] high reliability,[8] and small size.[9] The use of nuclear battery has become a good solution for the internal electricity supply of spacecrafts.[10,11] The nuclear batteries currently used in spacecrafts[12] and detectors[13] are mainly based on the radioisotope thermoelectric generator.[14,15] It loads ^{238}Pu source[16] and has a large volume generally,[17] and thus does not satisfy the small size demand. Radiovoltaic and radioluminescent nuclear batteries are superior in size, generally within 5 cm^3,[18,19] The mechanism of radiovoltaic nuclear battery is the direct collection of decay particles with semiconductor conversion units,[20,21] in which energy conversion efficiency (η) is ≈4%.[22] However, the direct contact of the semiconductor unit with the radioisotope source will cause serious damage,[23,24] which is not beneficial to achieve a stable output. Radioluminescent nuclear battery is based on radiovoltaic nuclear battery loading with a phosphor layer, as shown in **Figure 1**. The decay energy is first converted into light energy by phosphorous materials, and then electrical output is generated by photovoltaic units. This battery is expected to be a future candidate as an energy support system for space exploration and navigation missions.

At present, there are still several problems needed to be solved, such as the overall conversion efficiency, the service performance prediction, the damage of the phosphor layer, and the feasible optimized project. Its electrical property has been enhanced by matching the external quantum efficiency (EQE) with the radioluminescence spectrum,[25] and the mixing of the liquid radioisotope source and fluorescent materials is also a good idea.[26] However, its experimental η remains far from the calculated theoretical value of 7%,[27] radiation energy to light energy is about 20%,[28] light energy to electricity is about 35%.[29] Studies have explored the performance of some photovoltaic units under low light, such as silicon cells,[30] organic photovoltaics,[31] III–V semiconductor photovoltaics,[32] and thin-film CdTe/CdS solar cells.[33] All of them present an energy conversion difference

T. Jiang, C. Meng, Prof. X. Tang
Department of Nuclear Science and Technology
Nanjing University of Aeronautics and Astronautics
Nanjing 211106, China
E-mail: tangxiaobin@nuaa.edu.cn

Dr. Z. Xu, Dr. Y. Liu, Prof. X. Tang
Key Laboratory of Nuclear Technology Application and Radiation Protection in Astronautics
Ministry of Industry and Information Technology
Nanjing 211106, China

The ORCID identification number(s) for the author(s) of this article can be found under https://doi.org/10.1002/ente.202000667.

DOI: 10.1002/ente.202000667

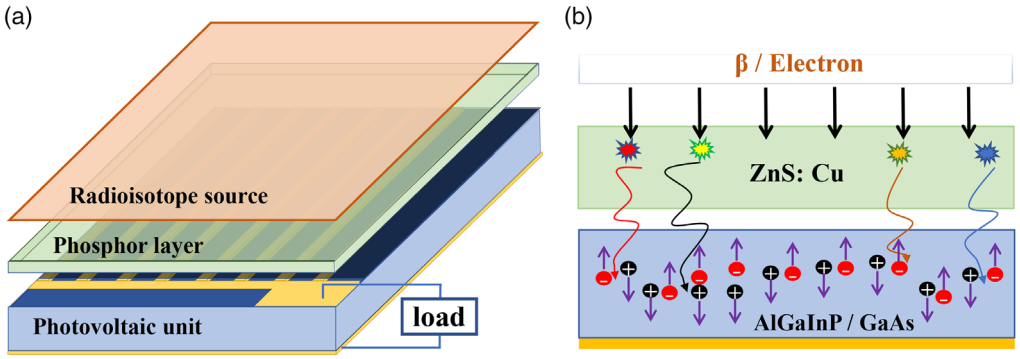

Figure 1. a) Diagram of the radioluminescent nuclear battery structure. b) Schematic of the radioluminescent nuclear battery.

under the low intensity of incident light. However, the light intensity of previous study is still too high to solve the problems in radioluminescent nuclear battery.

This study analyzed and compared the rule of the electrical properties of GaAs and AlGaInP photovoltaic units under different intensity levels of light, and proposed the minimum energy threshold of the radiation sources used in radioluminescent nuclear battery. The phosphor selected in this study was ZnS:Cu, which has good luminescence yield[34] and is radiation resistant.[35] The in situ electrical output of the battery under a high-intensity source was analyzed, which was excited by an electronic linear accelerator. This work used an electronic linear accelerator to replace the radiation sources by adjusting the beam energy to be equal to the average energy of radioisotopes, and obtained a high electron intensity by increasing the beam fluence. Furthermore, the radiation resistance of the phosphor layer was evaluated, providing important guidelines for improving electrical performance and optimizing solutions.

2. Experimental Section

The structure material of the radioluminescent nuclear battery in this research consists of three parts: 1) radioisotope sources, 2) the phosphor layer, and 3) semiconductor photovoltaic units.

2.1. Experimental Material

The radiation sources comprised eight ^{63}Ni radioisotopes with different activities and an electronic linear accelerator. The activities of the eight ^{63}Ni radioisotope sources were 2.29×10^7, 4.06×10^7, 7.02×10^7, 8.73×10^7, 9.49×10^7, 1.48×10^8, 1.78×10^8, and 2.40×10^8 Bq. All of them were round single-sided with a diameter of 15 mm. The ^{63}Ni is often used as the source of nuclear battery.[36] Other radioisotope sources were limited in use due to difficulties in preparation process.[37] The beam energy range of the electronic linear accelerator was 50–200 keV, which can replace the radioisotope sources with the same average energy.[22,38] The emission energy of 62 keV was used to replace the average energy of the ^{147}Pm.[39] The beam fluence intensity range was 5×10^8–2×10^{12} e cm^{-2} s^{-1}. The relationship between the activity of radioisotopes and the beam fluence intensity of the electron linear accelerator is shown in **Table 1**.

Table 1. Conversion relationship between the beam fluence of electron linear accelerator and the activity of radioisotope sources.

Beam fluence intensity [e cm^{-2} s^{-1}]	Activity [mCi cm^{-2}]
3.7×10^7	1
5×10^8	13.51
1.5×10^9	40.54
1×10^{10}	270.27
1×10^{11}	2702.70
1×10^{12}	27 027.03

To deposit all the energy, the phosphor layer was prepared with ZnS phosphor powder. The phosphor layers were 30×30 mm square film, and the layer thickness changed with the different radiation sources used.[35] In addition, substrate layers without phosphors were made with the same thickness as of the phosphor layer to analyze the effect of the substrate material on the emission of luminescence after irradiation. A 100 keV electron was used to irradiate the substrate and phosphor layers, and the total beam fluence values reached 2.16×10^{16} and 4.32×10^{16} e cm^{-2}, respectively.

There were two semiconductor photovoltaic conversion units of GaAs and AlGaInP. Both of them had antireflection coatings to reduce the light energy loss, and the size was 11×11 mm^2, thickness was about 1 mm. Both of them were produced in Shanghai Space Power Research Institute.

2.2. Experimental Methods

An adjustable monochromatic light source system, which the full width at half maximum (FWHM) of emission light was less than 10 nm was adopted for the performance testing of the photovoltaic units under various wavelengths. In addition, the diameter of the light spot emitted was about 1 mm, and would change slightly with the increasing of light energy intensity, which value was difficult to accurately measure. During the experiment, it was found that as long as the light spot can fall on the surface of the photovoltaic unit, the slight change of the light spot area

almost had no effect on its electrical output. Therefore, there were only light energy intensity without per unit area in the subsequent conclusions. The wavelength of monochromatic light was mainly 520 nm, which was the peak radioluminescence of ZnS:Cu. In addition, the performance changes of the three different wavelengths 393, 495, and 600 nm were also tested to study the relationship between the incident wavelength and the performance change.

The electrical properties of photovoltaic units and radioluminescent nuclear batteries were evaluated by a source meter (Keithley 2636A). The EQE of semiconductor photovoltaic units was analyzed by a spectral response/quantum efficiency measuring instrument. The electronic linear accelerator was used as a radiation source to obtain the high fluence intensity of the electron beam.

The phosphor and substrate layers were placed in the accelerator vacuum chamber for electron irradiation to explore the performance change after high influence electron radiation. In order to avoid extra radiation damage, an X-ray generator was used as the excitation source in the ex situ test. Radioluminescence spectra were obtained using an Agilent Technologies Cary Eclipse fluorescence spectrophotometer. The transmittance of the substrate layers was evaluated using an UV–visible spectrophotometer, which could analyze the attenuation caused by the nonphosphor powder, and put forward appropriate improvement solution.

3. Results and Discussion

3.1. Analysis of the Rule of Photovoltaic Conversion

Photoelectric conversion is a key link to radioluminescent nuclear batteries. The performance output rule of photovoltaic units under different light intensities and wavelengths must be analyzed.

3.1.1. Influence of Incident Light Intensity

The electrical performance tendency of the GaAs and AlGaInP photovoltaic units was analyzed under the changing intensities of incident light from dim to intense. The incident wavelength was 520 nm, and the electrical parameters are shown in **Figure 2**.

Figure 2a shows the photoelectric efficiency trend of AlGaInP and GaAs with the increasing light energy. The η of both photovoltaic units exhibits a sharp increasing tendency at the low incident intensity section. The incident light power of radioluminescent nuclear batteries was generally at the nW level,[34] explaining its low η. The η of the AlGaInP photovoltaic unit was ≈19.5% when the light power intensity was 1 μW. The enhancement of the overall efficiency tended to be slower, about 22% until the incident light was higher than 3 μW. The initial η value of the GaAs conversion unit was very low, nearly 0%,

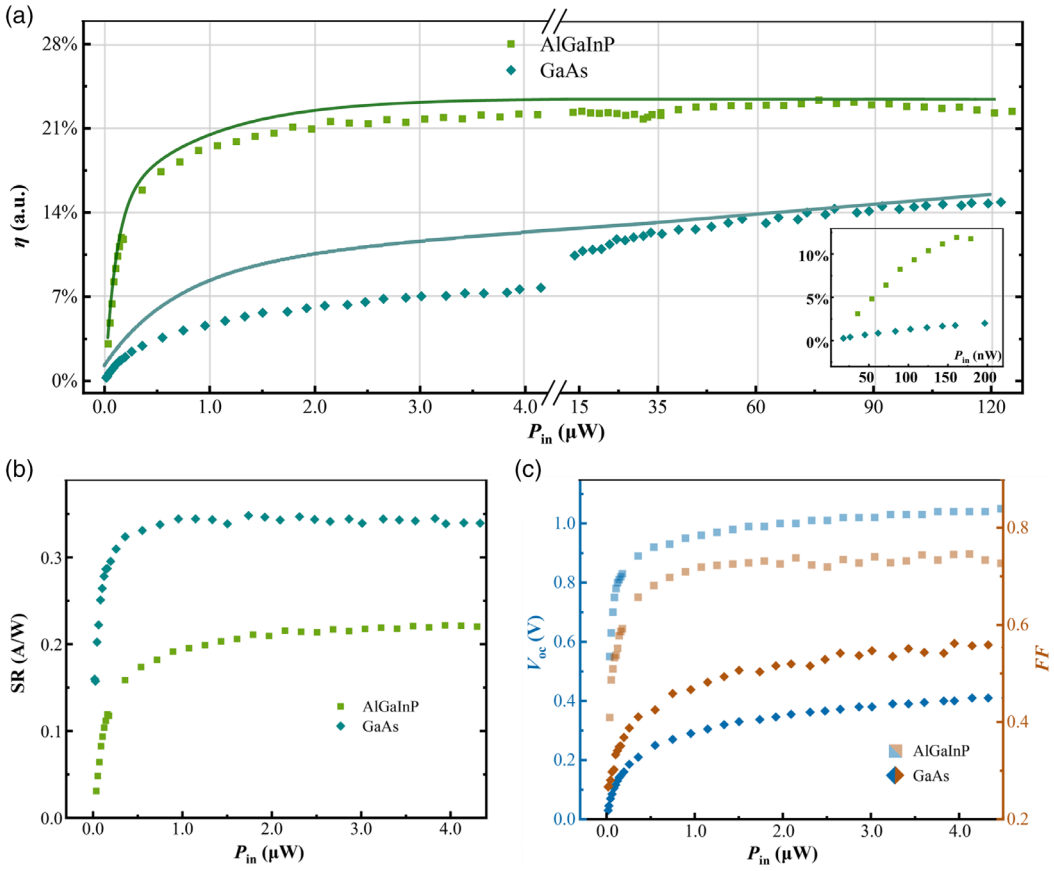

Figure 2. The electrical performance changing trend of GaAs and AlGaInP photovoltaic units under the light wavelength of 520 nm, as the intensity of incident light increases. a) Photoelectric conversion efficiency, b) spectral response (SR), c) open-circuit voltage (V_{oc}) and fill factor (FF).

but exhibited continuous growth with the increase in the light intensity. The efficiency reached 14.9% when the incident light intensity was 120 μW, and there was still an increasing tendency. It was considered that AlGaInP unit studied had a better electrical performance under dim light, and was more suitable as photoelectric conversion structure for radioluminescence compared with the GaAs unit. Therefore, the AlGaInP unit was adopted in subsequent studies on radioluminescent nuclear batteries. Figure 2b shows that the GaAs unit had a better SR than the AlGaInP unit, reaching an upper limit of about 1 μW and then maintaining stability at 0.339 A W^{-1}. However, the maximum SR value of AlGaInP unit could only reach 0.287 A W^{-1} under 520 nm monochromatic light. The initial V_{oc} of GaAs unit was only 0.03 V, and the FF was 0.267 when the incident light power was 17.7 nW. Furthermore, the band gap of GaAs is lower than that of AlGaInP semiconductor, and its voltage increase was slower. Under a stable SR, the increasing FF would cause every incident light energy to be converted into more electrical output, resulting in enhanced efficiency. Meanwhile, the AlGaInP unit exhibited constant FF and SR. The V_{oc} increased slightly, and the maximum value was limited by the bandgap of the semiconductor material,[27] which had little impact on the overall photoelectric conversion efficiency. Therefore, its η remained constant under high incident light energy.

The η improvement of the radioluminescent nuclear battery is inseparable from the energy intensity of the radioisotope sources. According to Figure 2, the incident light energy is at least 3 μW, which can ensure a high η of the AlGaInP units. If the radioluminescence conversion efficiency of the phosphor layer is 23%,[27] then the output power of the radioisotope sources needs to exceed 13 μW.

3.1.2. Influence of Incident Light Wavelength

The electrical property rule of AlGaInP unit at 520 nm wavelength light has been discussed. The other wavelengths with specific meanings are worth analyzing further. According to the EQE curve of AlGaInP unit, three wavelengths were selected as the research objective. The EQE value was the highest at 495 nm, reaching 70%, and the value was 50% at 393 and 600 nm, as shown in **Figure 3**. The electrical performance rule under different intensities was discussed at these three wavelengths.

The GaAs unit has a wider quantum response wavelength range and a higher EQE value than the AlGaInP unit, which are more suitable for absorbing the solar energy conversion of sunlight.[5,40] Although the EQE curve shows that the GaAs unit has a good performance parameter, the η will not be high enough because of its narrow bandgap and low V_{oc}. Figure 3b,c show the trends of η and SR at different wavelengths with increasing incident power. All of them show a unified variation tendency and the same rise curve under 393 and 600 nm incident lights. It can be considered that one photovoltaic unit will show the same

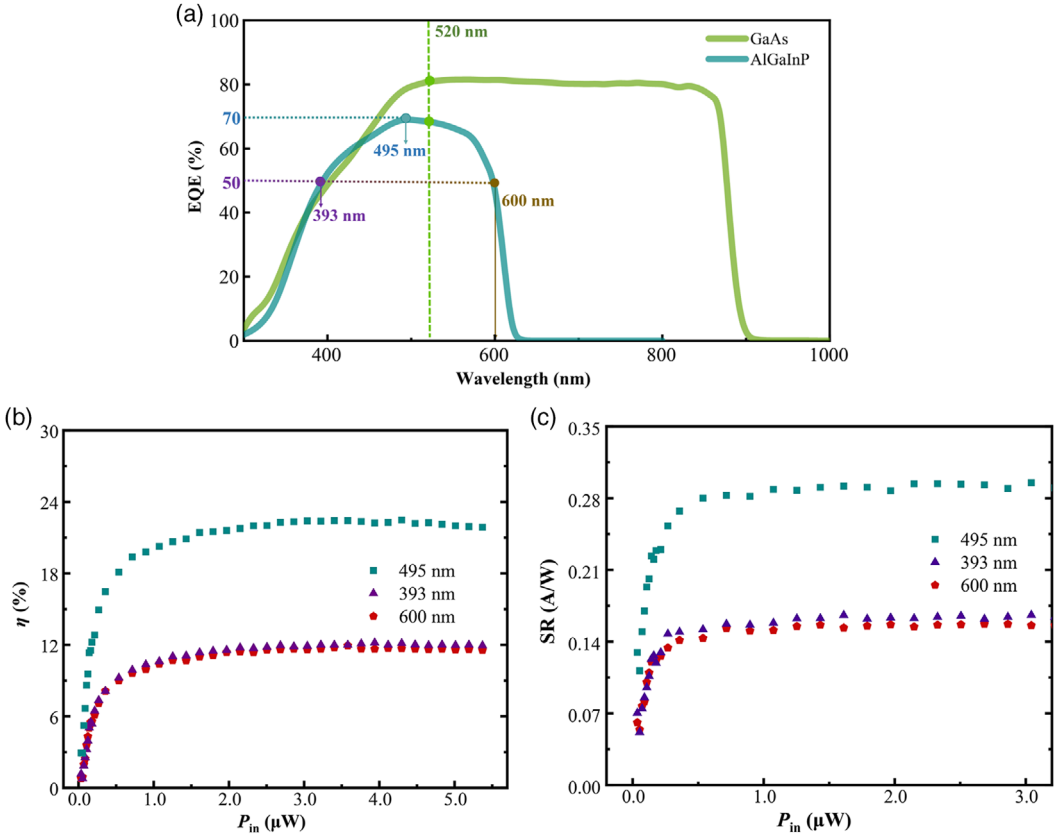

Figure 3. a) EQE curves of GaAs and AlGaInP photovoltaic units. Under three wavelengths of monochromatic light, b) the η changes rule of AlGaInP photovoltaic unit, c) the spectral response changes rule of AlGaInP photovoltaic unit with the increasing light intensity.

sensitivity variation trend of photovoltaic response at different wavelengths. The EQE will only affect the maximum value of η. There was a 28% drop in EQE value at different wavelengths. But the drop increased to about 50% when the difference was reflected on η and SR. It indicates that the η is highest only at the peak wavelength of EQE curve, and the performance degradation at other wavelength positions are more severe than the decrease in the quantum response sensitivity.

The performance rules of photovoltaic units provide guidance for the phosphor layer and radioisotope source used in radioluminescent nuclear battery. The radioluminescence spectrum of the phosphor layer should be located at the peak of the EQE curve to maximize the use of energy. There are incident light intensity threshold values of semiconductor photovoltaic units. Only when the incident light energy is above the threshold, it will present a good and stable η. In addition, the threshold value of incident light energy is only related to the semiconductor material of photovoltaic unit, and will not be affected by the wavelength of incident light. The incident energy threshold of GaAs unit studied is so high that greater than 120 μW; that of AlGaInP unit is only 3 μW, which is considered more suitable for radioluminescent nuclear battery to obtain the high efficiency under dim light intensity.

3.2. Analysis of Radioluminescent Nuclear Battery Performance

The aforementioned studies have explored the output rule of AlGaInP unit under dim and intense lights, and the conclusions obtained could be introduced into radioluminescent nuclear battery. Then, the electrical output performance under different activities of ^{63}Ni dim radiation sources and electronic linear accelerator intense sources were explored.

3.2.1. Electrical Properties under Dim Radiation Sources

The relationship between the ^{63}Ni radioisotope sources of different activities and the electrical output was studied. The thickness of the phosphor layer was about 55 μm. The maximum power (P_{max}) and η parameters are shown in **Figure 4**.

The green point in Figure 4 represents the electrical output at a certain activity of ^{63}Ni. The P_{max} of the battery shows a steadily increasing trend with the increasing activity. The slope of the connection line between each green point and the original point is the conversion efficiency at this activity. The blue dotted line represents the η of the battery, which is 0.6%. The points above the line indicate that the η is greater than 0.6%, and vice versa. The tendency corresponds with the photovoltaic unit tested under dim and intense lights, indicating that the photoelectric conversion rule obtained is also applicable in radioluminescent nuclear battery. By combining the parameter information in Figure 4 and the conclusion obtained in Figure 2a, the efficiency of converting radiation energy to luminescence energy was calculated to be ≈10%. Only when the activity of the ^{63}Ni radioisotope sources was greater than 250.8 mCi cm^{-2}, it is time that the energy of the incident light reaches the threshold of AlGaInP unit calculated earlier. It is a very high value, and difficult to prepare based on the current manufacturing process.[41] In summary, high radiation intensity is a prerequisite for high-performance battery

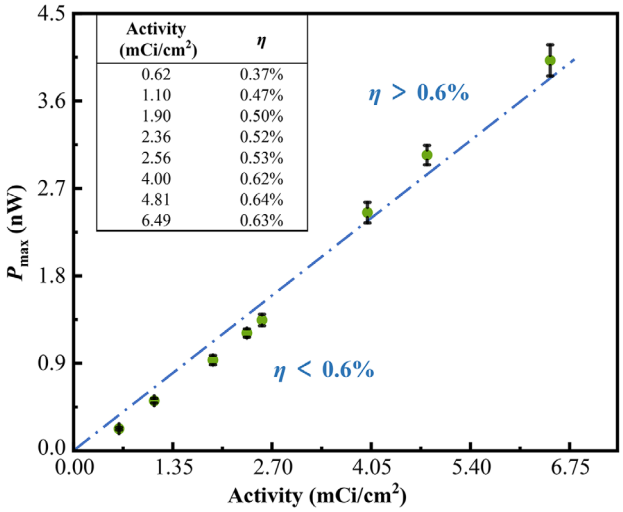

Figure 4. The P_{max} tendency and η of radioluminescent nuclear battery with eight different radioisotopes.

output. According to the advantages of adjustable beam energy and beam fluence intensity, an electronic linear accelerator was used as a high-activity radiation source.

3.2.2. Electrical Properties under Intense Radiation Sources

The average energy of the ^{147}Pm radioisotope source is 62 keV, and the emission beam energy of the electronic linear accelerator was adjusted to this value to replace the high-activity ^{147}Pm sources. To deposit all the energy of the electrons in the phosphor layer, the thickness of phosphor layer was about 150 μm. The output electrical parameters under different beam intensities are shown in **Table 2**.

Three beam intensities were adopted, and each point had series and parallel connections. The results satisfy the Ohm's law. The overall output power and the conversion efficiency of the series connections are slightly higher than those of the parallel connections. It is because the internal differences of photovoltaic units cause more energy loss under parallel connection than under the series connection. According to several sets of output parameters, the V_{oc} and FF are enhanced with increasing beam fluence intensity, which is consistent with the conclusion obtained in Figure 2. By combining the P_{max}

Table 2. Electrical output parameters with the electron energy of 62 keV under different beam fluence intensities.

Beam fluence intensity [e cm^{-2} s^{-1}]	Connection mode	P_{max} [nW]	I_{sc} [nA]	V_{oc} [V]	FF	η [%]
5×10^8	Series	88.39	78.6	1.63	0.69	0.73
	Parallel	83.45	145.6	0.88	0.65	0.69
1.5×10^9	Series	283.10	216.6	1.85	0.71	0.78
	Parallel	272.89	395.4	0.94	0.73	0.76
1×10^{10}	Series	2075.19	1192.1	2.34	0.74	0.87
	Parallel	1991.04	2097.8	1.24	0.77	0.83

of the series connection of AlGaInP photovoltaic units at the 5×10^8 e cm^{-2} s^{-1} in Table 2 and the parameter data in Figure 2, the incident radioluminescence intensity was calculated to be 252.5 nW cm^{-2}. The photoelectric η was 14.4%, and the power of radiation source was about 4.96 μW cm^{-2}, so the efficiency of converting the radiation energy to light energy was only 5%. It was considered that the thickening of the phosphor layer would hinder photon emission and introduced more self-absorption, reducing the η of radiation energy to light energy. When the beam fluence intensity was 1.5×10^9 e cm^{-2} s^{-1}, the incident optical power was estimated at 640.2 nW cm^{-2}, and photoelectric η was 18.2%. The radioluminescence efficiency was about 4.3%. When the beam fluence intensity was 1×10^{10} e cm^{-2} s^{-1}, the photoelectric efficiency stabilized at 22%, and the incident optical power exceeded 3 μW. The η of the radioluminescence was 3.9% at this time. Although the overall efficiency of the radioluminescent nuclear battery continued to increase, the radioluminescence degradation had occurred.

As the enhancement of the electron beam fluence intensity, the electrical output of the radioluminescent nuclear battery exhibited a more significant decline, as shown in **Figure 5**. The beam fluence intensity of the radiation source had reached 1×10^{11} e cm^{-2} s^{-1}, indicating that the emission energy of electrons was 992 μW cm^{-2}. It could be seen from the *I–V* curve and the electrical performance parameters in Figure 5, shows that the severe decrease was not only caused by the radiation damage to phosphor layer but also by the performance failure of the photovoltaic units under such a strong electromagnetic pulse radiation field. The V_{oc} of AlGaInP unit no longer increased regularly with the increasing beam fluence intensity. It was considered that the electrons were enriched on the surface of the printed circuit board (PCB) behind the photovoltaic unit, interfering with the conductive property of the gold wire and the solder joints, causing Ohmic contact degradation, and leading to battery degradation.[42] Therefore, it was believed that extremely intense radiation sources would cause the failure of the radioluminescent nuclear battery. In this experiment, the 1×10^{10} e cm^{-2} s^{-1} fluence was the best intensity, allowing the battery to obtain good performance parameters.

3.3. Performance Attenuation Caused by Radiation Sources

The performance attenuation rule and mechanism of the phosphor layer which directly exposed to the electron radiation must be studied further. The excitation source used for experimental testing was an X-ray generator with a low linear energy transfer (LET),[23] to avoid introducing additional radiation damage to the phosphor layer during the ex situ performance test.

3.3.1. Performance Attenuation of the Phosphor Layer

The luminescence emission of the phosphor layer is the key to the output stability of radioluminescent nuclear battery. The optical and electrical performance are shown in **Figure 6**.

The emission spectrum of the ZnS:Cu phosphor was just suitable for the quantum response curve of AlGaInP unit shown in Figure 3a. The three radioluminescence spectra maintained the same shape in Figure 6a, and only the peak intensity decreased. The peak wavelength of the radioluminescence spectrum did not shift, indicating that the electron irradiation did not introduce other energy levels that could produce luminescence photons. The FWHM of the spectra did not change significantly; it was considered that the phosphor grains in the phosphor layer did not swell after electron irradiation.[35] The optical property dropped by 6.6% and 14.2% at the two radiation fluence intensities, respectively. The electrical performance is shown in Figure 6b, which attenuation trend was similar to the optical property. The P_{max} had decreased by 8.5% and 15.2%, respectively. The decrease in electrical intensity was higher than that in optical intensity; it was because the incident energy of the luminescence was less than the threshold value of 3 μW, and the photoelectric efficiency decreased with the drop of incident light energy in this energy range.

3.3.2. Factors of Performance Attenuation

There are some previous researches find that the phosphor has an excellent radiation resistance, and exhibits minimal property degradation under high-energy electron irradiation.[43,44] Therefore, investigating the performance of the substrate material after irradiation is also important. The appearance of the phosphor layers and the transmittance of the substrate layer after irradiation are shown in **Figure 7**.

It could be seen intuitively that the irradiated phosphor layers showed a clear yellowing tendency; it was believed that the color center effect caused by the substrate material after radiation, generating light traps, and reducing the light output.

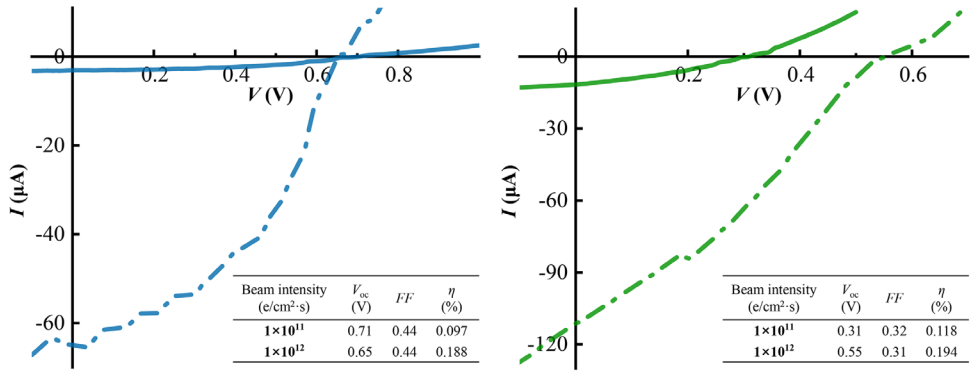

Figure 5. *I–V* curves of the two AlGaInP units above covered phosphor layer under the beam fluence intensity of 1×10^{11} and 1×10^{12} e cm^{-2} s^{-1}.

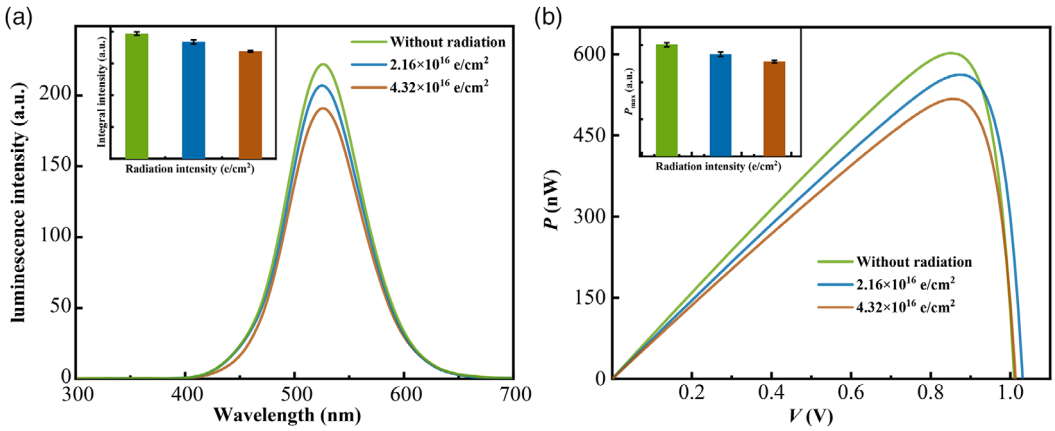

Figure 6. a) Radioluminescence spectrum of the phosphor layer and the decrease in the luminescence integral intensity after electron irradiation. b) *P*–*V* curves and P_{max} trend of the phosphor layer loaded on the AlGaInP photovoltaic unit.

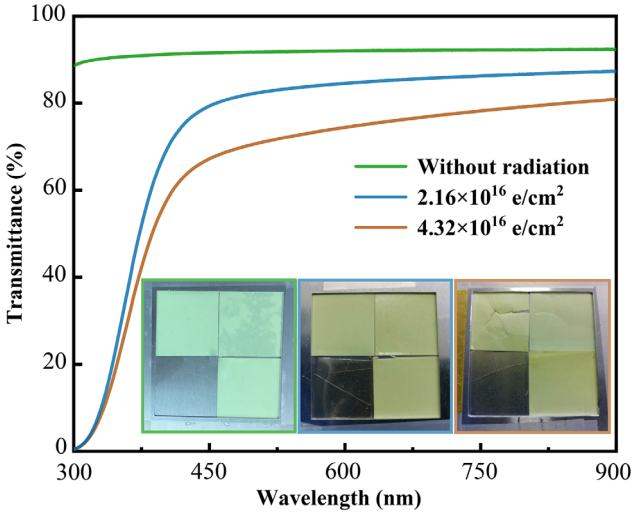

Figure 7. The appearance of phosphor layers and the transmittance of the substrate layer after electron radiation.

The transmittance continued to drop with the increasing beam fluence intensity. The substrate layer transmittance was near 90% between 300 and 900 nm without radiation. After being irradiated with electrons, the transmittance of the photons in the ultraviolet wavelength was very low, which was close to 0% at the wavelength of 300 nm. For the radioluminescent nuclear battery in this study, the green light near 520 nm is the main area of interest. The transmittance of substrate layer at 520 nm dropped by 22.3% when the beam fluence intensity reached 4.32×10^{16} e cm^{-2}. This decrease was greater than the attenuation of the optical property of the phosphor layer at the same dose. It is because the radioluminescence photons is generated inside the phosphor layer; the transmittance value only reflects a trend of the photon transmission of the phosphor layer but cannot accurately obtain the photon emission.

The microscopic morphology changes of the phosphor layers after radiation are worth exploring with SEM, as shown in **Figure 8**. It could be seen that the surface of the phosphor layer without radiation was very smooth, and the small raised particles were the blended ZnS:Cu grains. Figure 8b shows that the phosphor layer agglomerated slightly on the surface when the beam fluence intensity reached 2.16×10^{16} e cm^{-2}. The agglomeration enhanced the self-absorption of phosphor and hindered the emission of luminescence photons. Figure 8c shows that the surface of phosphor layer was damaged severely, forming a larger size and a greater number of agglomerations, when the radiation beam fluence intensity was 4.32×10^{16} e cm^{-2}. Furthermore, some cracks appeared on the surface, and agglomerations tended to gather near the cracks. It was considered that electron radiation simultaneously produced the thermal effect, which caused

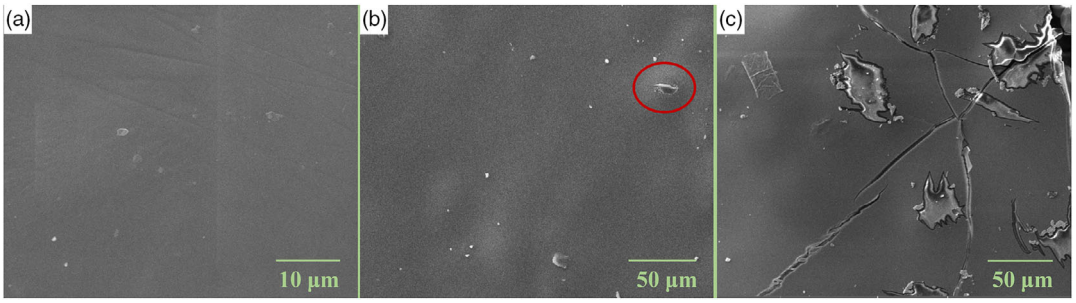

Figure 8. SEM images of the phosphor layer a) without radiation. The cumulative radiation beam fluence intensity b) 2.16×10^{16} e cm^{-2}, c) 4.32×10^{16} e cm^{-2}.

molecules of the substrate layer to expand under radiation and heat. The crack was formed to release the stress between molecules, so cracks are prone to occur at the areas where the agglomeration is dense, or crack directly at the agglomeration. The main reason for the attenuation of the phosphor layer after irradiation is that the emission of radioluminescence is blocked by the substrate layer damage.

4. Conclusion

The study explored the radioluminescence and photoelectric energy conversion mechanism of radioluminescent nuclear battery, to balance and improve its output power and energy conversion efficiency. When the incident photon energy was ≈100 nW, the η of the AlGaInP and GaAs units were 9.35% and 1.31%, respectively. Only when the incident light energy reached a certain threshold value, did the photovoltaic units maintained the maximum sensitivity of quantum response. Results show that the incident energy threshold was mainly related to the material of the semiconductor photovoltaic unit, and not affected by wavelength change. The threshold of AlGaInP photovoltaic unit is 3 μW, with a maximum efficiency of 22%. The threshold of GaAs photovoltaic unit is higher than 120 μW, where the η is about 14.9%. Therefore, the AlGaInP unit is more suitable for radioluminescent nuclear battery, because of its high efficiency in dim light. The ZnS:Cu phosphor layer and AlGaInP photovoltaic unit load with ^{63}Ni sources with the activity of 4.81 mCi cm^{-2} to form radioluminescent nuclear batteries, which can achieve a maximum efficiency of 0.64%. When the electronic linear accelerator was used to replace the ^{147}Pm with an activity of 270.27 mCi cm^{-2}, the overall η of the battery reached 0.87%. This activity value is very high, indicating advanced requirements for the preparation of radioisotope sources. However, if the intensity of the radiation source is extremely high, it will lead to a failure of the battery. Moreover, a high intensity can introduce the color center effect and agglomeration cracks on the surface of the phosphor layers, which will result in the transmittance reduction of the substrate layer at the radioluminescence wavelengths. This phenomenon eventually leads to a drop in the output electric power of radioluminescent nuclear battery. The radioluminescence emission and performance optimization of the phosphor layer is worth to exploring deeply in future.

Acknowledgements

This work was supported by the National Natural Science Foundation of China (grant no. 11675076), National Natural Science Foundation of China (grant no. 12005101), and China Postdoctoral Science Foundation (grant no. 2019M661836).

Conflict of Interest

The authors declare no conflict of interest.

Keywords

nuclear batteries, photovoltaic energy conversion, radiation degradation, radioluminescence

Received: July 20, 2020
Revised: September 29, 2020
Published online: October 14, 2020

[1] M. S. Elgenk, *Energy Convers. Manage.* **2008**, *3*, 381.
[2] R. J. Cassady, R. H. Frisbee, J. H. Gilland, M. Houts, M. R. Lapointe, C. M. Maressereading, S. R. Oleson, J. E. Polk, D. Russell, A. Sengupta, *Energy Convers. Manage.* **2008**, *49*, 412.
[3] T. George, in *Proc. of Smart Sensors, Actuators, and MEMS*, SPIE **2003**, pp. 136–148.
[4] M. Yamaguchi, *Sol. Energy Mater. Sol. Cells* **2003**, *75*, 261.
[5] W. Rong, G. Zengliang, Z. Xinghui, Z. Zuoxu, *Sol. Energy Mater. Sol. Cells* **2003**, *77*, 351.
[6] G. Li, Y. Yang, R. A. Devine, C. Mayberry, *Nanotechnology* **2008**, *19*, 424014.
[7] G. A. Landis, S. G. Bailey, E. B. Clark, M. G. Myers, M. F. Piszczor, M. S. Murbach, in *2012 38th IEEE Photovoltaic Specialists Conf.*, IEEE **2012**, pp. 002819–002824.
[8] R. G. Lange, W. P. Carroll, *Energy Convers. Manage.* **2008**, *49*, 393.
[9] L. C. Olsen, P. Cabauy, B. J. Elkind, *Phys. Today* **2012**, *65*, 35.
[10] G. R. Schmidt, R. L. Wiley, R. L. Richardson, R. R. Furlong, in *AIP Conf. Proc.*, Vol. *746*, American Institute of Physics **2005**, pp. 429–436.
[11] G. L. Bennett, *Energy Convers. Manage.* **2008**, *49*, 382.
[12] R. C. Obrien, R. M. Ambrosi, N. P. Bannister, S. D. Howe, H. V. Atkinson, *J. Nucl. Mater.* **2008**, *377*, 506.
[13] F. Ritz, C. E. Peterson, in *2004 IEEE Aerospace Conf. Proc.*, IEEE **2004**, Vol. *5*, pp. 2950–2957.
[14] K. Liu, X. Tang, Y. Liu, Z. Yuan, J. Li, Z. Xu, Z. Zhang, W. Chen, *J. Power Sources* **2018**, *393*, 161.
[15] Z. Yuan, X. Tang, Y. Liu, Z. Xu, K. Liu, J. Li, Z. Zhang, H. Wang, *J. Power Sources* **2019**, *414*, 509.
[16] O. Artun, *Appl. Radiat. Isot.* **2020**, *166*, 109337.
[17] M. S. Elgenk, H. H. Saber, *Energy Convers. Manage.* **2006**, *47*, 2290.
[18] Z. Xu, X. Tang, Y. Liu, Z. Zhang, W. Chen, K. Liu, Z. Yuan, *ACS Appl. Mater. Interfaces* **2019**, *11*, 14191.
[19] Y. Liu, X. Tang, Z. Xu, L. Hong, P. Wang, D. Chen, *Sci. China-Technol. Sci.* **2014**, *57*, 14.
[20] M. Lu, G. Zhang, K. Fu, G. Yu, D. Su, J. Hu, *Energy Convers. Manage.* **2011**, *52*, 1955.
[21] C. J. Eiting, V. Krishnamoorthy, S. Rodgers, T. George, J. David Robertson, J. D. Brockman, *Appl. Phys. Lett.* **2006**, *88*, 064101.
[22] M. R. Khan, J. R. Smith, R. P. Tompkins, S. Kelley, M. Litz, J. Russo, J. Leathersich, F. Shahedipoursandvik, K. A. Jones, A. A. Iliadis, *Solid-State Electron.* **2017**, *136*, 24.
[23] G. A. Umanamembreno, J. Dell, T. P. Hessler, B. Nener, G. Parish, L. Faraone, U. K. Mishra, *Appl. Phys. Lett.* **2002**, *80*, 4354.
[24] G. P. Summers, E. A. Burke, P. Shapiro, S. R. Messenger, R. J. Walters, *IEEE Trans. Nucl. Sci.* **1993**, *40*, 1372.
[25] L. Hong, X. Tang, Z. Xu, Y. Liu, D. Chen, *Phys. Res. Sect. B* **2014**, *338*, 112.
[26] J. Russo, M. Litz, W. B. Ray, B. Smith, R. Moyers, *Appl. Radiat. Isot.* **2017**, *130*, 66.
[27] *Polymers, Phosphors, and Voltaics for Radioisotope Microbatteries*, (Eds: K. E. Bower, Y. A. Barbanel, Y. G. Shreter, G. W. Bohnert), CRC Press, Boca Raton, FL **2002**.
[28] M. S. Litz, D. C. Katsis, J. A. Russo, J. J. Carroll, in *Energy Harvesting and Storage: Materials, Devices, and Applications V*, Vol. *9115*, International Society for Optics and Photonics **2014**, p. 91150J.
[29] W. Shockley, H. J. Queisser, *J. Appl. Phys.* **1961**, *32*, 510.
[30] N. H. Reich, W. G. Van Sark, E. A. Alsema, R. W. Lof, R. E. I. Schropp, W. C. Sinke, W. C. Turkenburg, *Sol. Energy Mater. Sol. Cells* **2009**, *93*, 1471.

[31] R. Steim, T. Ameri, P. Schilinsky, C. Waldauf, G. Dennler, M. C. Scharber, C. J. Brabec, *Sol. Energy Mater. Sol. Cells* **2011**, *95*, 3256.
[32] J. Russo, W. B. Ray, M. Litz, *Appl. Energy* **2017**, *191*, 10.
[33] D. Shvydka, V. G. Karpov, A. D. Compaan, *Appl. Phys. Lett.* **2003**, *82*, 2157.
[34] Z. Xu, Y. Liu, Z. Zhang, W. Chen, Z. Yuan, K. Liu, X. Tang, *Int. J. Energy Res.* **2018**, *42*, 1729.
[35] T. Jiang, Z. Xu, X. Tang, Z. Yuan, H. Wang, M. Bian, *Int. J. Energy Res.* **2020**, https://doi.org/10.1002/er.5526.
[36] O. Artun, *Int. J. Mod. Phys. E* **2019**, *28*, 19300066.
[37] O. Artun, *Appl. Phys. A* **2020**, *126*, 386.
[38] A. Sharma, J. Melancon, S. G. Bailey, S. Zivanovic, *IEEE Trans. Electron Devices* **2015**, *62*, 2320.
[39] O. Artun, *Indian J. Phys.* **2017**, *91*, 909.
[40] F. Dimroth, M. Grave, P. Beutel, U. Fiedeler, C. Karcher, T. N. D. Tibbits, E. Oliva, G. Siefer, M. Schachtner, A. Wekkeli, A. W. Bett, R. Krause, M. Piccin, N. Blanc, C. Drazek, E. Guiot, B. Ghyselen, T. Salvetat, A. Tauzin, T. Signamarcheix, A. Dobrich, T. Hannappel, K. Schwarzburg, *Prog. Photovoltaics* **2014**, *22*, 277.
[41] J. Russo, M. Litz, W. B. Ray, G. M. Rosen, D. I. Bigio, R. Fazio, *Appl. Radiat. Isot.* **2017**, *125*, 66.
[42] S. Kayali, *Microelectron. Reliab.* **1999**, *39*, 1723.
[43] K. K. Babitha, K. P. Priyanka, A. Sreedevi, S. Ganesh, T. Varghese, *Ceram. Int.* **2019**, *45*, 2576.
[44] S. Brunner, W. Puff, A. G. Balogh, P. Mascher, *Phys. B* **1999**, *273*, 898.